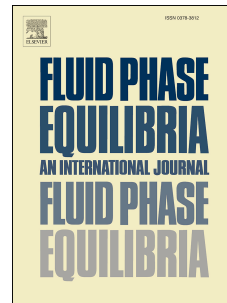


Accepted Manuscript

A comparative analysis of thermophysical properties correlations for n-paraffins to be used in wax precipitation modeling

Priscila R. Kazmierczak, Márcio L.L. Paredes, Eduardo R.A. Lima, J.A.P. Coutinho



PII: S0378-3812(18)30198-5

DOI: [10.1016/j.fluid.2018.05.012](https://doi.org/10.1016/j.fluid.2018.05.012)

Reference: FLUID 11834

To appear in: *Fluid Phase Equilibria*

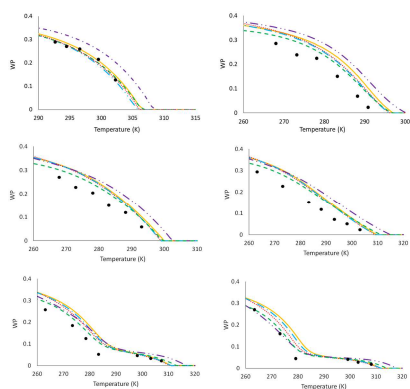
Received Date: 22 February 2018

Revised Date: 28 April 2018

Accepted Date: 11 May 2018

Please cite this article as: P.R. Kazmierczak, Má.L.L. Paredes, E.R.A. Lima, J.A.P. Coutinho, A comparative analysis of thermophysical properties correlations for n-paraffins to be used in wax precipitation modeling, *Fluid Phase Equilibria* (2018), doi: 10.1016/j.fluid.2018.05.012.

This is a PDF file of an unedited manuscript that has been accepted for publication. As a service to our customers we are providing this early version of the manuscript. The manuscript will undergo copyediting, typesetting, and review of the resulting proof before it is published in its final form. Please note that during the production process errors may be discovered which could affect the content, and all legal disclaimers that apply to the journal pertain.



ACCEPTED MANUSCRIPT

A comparative analysis of thermophysical properties correlations for n-paraffins to be used in wax precipitation modeling

PRISCILA R. KAZMIERCZAK^{1,2}, MÁRCIO L. L. PAREDES^{1,*}, EDUARDO R. A. LIMA¹, COUTINHO, J. A. P.³

¹ Programa de Pós-Graduação em Engenharia Química, Universidade do Estado do Rio de Janeiro - UERJ, CEP 20550-013, Rio de Janeiro, RJ, Brazil.

² Agência Nacional do Petróleo – ANP, CEP 20090-003, Rio de Janeiro, RJ, Brazil.

³ CICECO – Aveiro Institute of Materials, Department of Chemistry, University of Aveiro, 3810-193 Aveiro, Portugal

Abstract

The performance of a thermodynamic wax precipitation model strongly depends upon the n-paraffin thermophysical properties used. In order to estimate them, several correlations have been proposed, and their values have a great impact on both calculated wax disappearance temperature (WDT) and amount of wax precipitated at each temperature (WPC). The main goal of this work is to evaluate the correlations available for the relevant thermophysical properties aiming at achieving a reliable wax precipitation modelling. The methodology used involves the direct comparison of the correlations with the values of pure n-paraffin properties, and indirect evaluation by their use in the estimation of wax disappearance temperatures, the amount of wax precipitated at each temperature, and DSC experimental curves. This study contemplates two thermodynamic approaches for paraffin precipitation: the solid solution (SS), which considers the formation of one solid solution; and the multisolid phase model (MS), that assumes that each solid phase consists of a pure component.

Keywords: n-paraffin properties, wax precipitation, correlations analysis.

Introduction

Wax precipitation is a common problem in oil industry. In order to predict it several thermodynamic models were proposed in the last 30 years. There are two main approaches to describe the solid phase. The first approach proposed considers the formation of one solid solution [1-4], later evolving to models that allow multiple solid solutions [5,6]. The second approach is based on the hypothesis that the solid phase is formed by several independent pure solid phases [7].

For the use of these thermodynamic models, data for several thermophysical properties, such as temperatures and enthalpies of fusion and of solid-solid transition, are required. If the thermodynamic model represents the liquid phase by a fugacity coefficient, it is also necessary to know the critical properties. These properties are used in the

calculation, e.g., of wax disappearance temperature (WDT) and the amount of wax precipitated at each temperature (WPC).

A large amount of experimental data for the properties of pure n-alkanes is found in the literature, and over the years, several correlations were proposed relating them with the carbon numbers of n-alkanes. Some of these correlations were directly developed for wax precipitation models, like the correlations proposed by Pedersen and Skovborg (1991) [3], that modified the correlations for solid-solid enthalpy of transition and heat capacities differences between solid and liquid phases, used by Won (1986) [1], with factors fitted to reproduce experimental wax precipitation data of North Sea oils. However, most works attempted to keep the properties of the pure n-alkanes on their modelling.

Some authors [8-12] suggest the use of different correlations depending upon carbon chain sizes. Ji. et al. (2004) [10] and Tabatabaei-Nejad and Khodapanah (2009) [13] also proposed the use of different correlations for odd and even carbon numbers. The argument is based on experimental data, since melting enthalpies variations as a function of carbon atom number show an odd-even effect [14-16].

Another aspect of the n-alkanes rich phase behavior is the existence of several solid phases that can be divided into four main groups: rotator, triclinic, monoclinic and orthorhombic [17,18]. Rotator phases permit molecular rotation. This behavior is not present in other phases, that will be called here ordered phases. Despite of the existence of several solid-solid transitions, thermal effects are prominent only on rotator-ordered phase transition [14,19]. Thus, this phase transition must be considered in order to reproduce a calorimetric curve. However, most thermodynamic models disregard this transition. Won (1986, 1989) [1-2] ignored the solid-solid transition. Coutinho and Stenby (1996) [4] and Coutinho (1998) [5] assumed that the precipitation usually occurs at a temperature below the solid-solid transition, thus the wax would present an orthorhombic structure. We refer to this approach as solid solution (SS). The approach proposed by Heidemann (2005) [6] enables, however, two solid structures: the rotator and the orthorhombic.

In the present work, the solid-solid transition will be considered only for the multisolid phase model (MS). In this case the solid phases are assumed to be pure, and are considered in a rotator form when the temperature is above the solid-solid transition temperature for that component, or otherwise in an orthorhombic phase. The solid-solid transition on SS model and the possibility of formation of multiple solid solutions are being studied in order to consider these particularities in future model developments.

Matheson and Smith (1985) [20] reported that a chain size difference of around 22% is the limit to form a continuous series of solid solution. However, for n-paraffins with low molecular weight, little size differences might lead to the formation of eutectic systems, as observed by Mondieig et al. (2004) [21] for the octane + decane mixture. On the other hand, in order to form a eutectic system in mixtures of n-paraffins with large molecular weight, this difference has to be significantly larger, as observed by Petitjean et al. (2002) [22] for pentacontane-pentacosane and for pentacontane-tricosane mixtures and also by Gilbert et al. (1996) [23] for eicosane-hexatriacontane mixture. Hence, the mixtures chosen in this work to represent the SS approach have small

differences in the size of its components, while the MS approach will be applied to mixtures with large differences among chain sizes.

The aim of this work is to select the best sets (ensembles) of correlations for the thermodynamic modeling of wax precipitation, considering both the solid solution and the multisolid phase approaches. For this purpose a set of experimental data will be selected for benchmarking, and the correlations detailed below are evaluated using the various thermodynamic models here adopted.

Thermodynamic modeling

The criterion for solid-liquid thermodynamic equilibrium is the equality of the fugacities of each compound in the solid and liquid phases. Solid-liquid equilibrium of pure components can be calculated by Equation (1) that relates the fugacities on liquid and solid phases with the thermophysical properties of pure components [24].

$$f_{i,pure}^S(P,T) = f_{i,pure}^L(P,T) \exp \left[\frac{\Delta^f H_i}{RT_i^f} \left(1 - \frac{T_i^f}{T} \right) + \frac{\Delta^t H_i}{RT_i^t} \left(1 - \frac{T_i^t}{T} \right) + \frac{\Delta^f C p_i}{R} \left(\frac{T_i^f}{T} - \ln \left(\frac{T_i^f}{T} \right) - 1 \right) \right] \quad (1)$$

where $f_{i,pure}^S(P,T)$ is the fugacity of pure component i in the solid phase at reference pressure P and temperature T ; $f_{i,pure}^L(P,T)$ is the fugacity of pure component i in the liquid phase; $\Delta^f H_i$ and $\Delta^t H_i$ are the fusion enthalpy and solid-solid transition enthalpy of component i ; T_i^f and T_i^t are the fusion and solid-solid transition temperatures; $\Delta^f C p_i$ is the difference in specific heat capacity between solid and liquid phases of pure component i ; and R is the gas universal constant.

Taking the liquid as the reference phase, the partition coefficient is defined by Equation (2).

$$K_i = \frac{x_i^L}{x_i^S} = \frac{\gamma_i^S}{\gamma_i^L} \psi_i = \frac{\gamma_i^S \phi_i^L}{\hat{\phi}_i^L} \psi_i \quad (2)$$

where K_i is partition coefficient of component i ; x_i^L and x_i^S are the molar fraction of component i in the liquid and solid phases; γ_i^S and γ_i^L are the activity coefficients of component i in the solid and liquid phases; ψ_i is the fugacity ratio between pure component i in solid and liquid phases; ϕ_i^L is the fugacity coefficient of pure component i ; and $\hat{\phi}_i^L$ is the fugacity coefficient of component i in the liquid solution.

Equations (1) and (2) are fundamental to describe the wax precipitation for both MS and SS approaches.

Additionally, in the SS approach a flash algorithm with the Rachford-Rice equation (Equation (3)) is required for modeling the equilibria.

$$\sum_i \frac{z_i(K_i - 1)}{1 + S(K_i - 1)} = 0 \quad (3)$$

where z_i is the global composition of component i and S is the solid phase ratio.

On the other hand, in the multisolid approach no flash algorithm is required, because the solid phases are supposed to be pure. However, it is required a stability analysis to describe the precipitation of each component. This stability criterion is expressed by Equation (4) [25].

$$\widehat{f}_i(P, T, z) - f_i^s(P, T) \geq 0 \quad (4)$$

According to this model, if the fugacity of the pure component in the solid phase ($f_i^s(P, T)$) is lower than its fugacity in the liquid mixture at global composition ($\widehat{f}_i(P, T, z)$), it will exist as a pure solid phase.

The equations exposed on this section, together with mass balance equations are able to predict the precipitation phenomena for both approaches.

The modeling of calorimetric curve was explained in a previous work [26], and follows in Equation (5) (MS) or Equation (6) (SS).

$$\begin{aligned} DSC_{\text{theoretical}} = & \left(- \sum_i \Delta_i^p H \cdot S_i - \sum_{i, T < T_i^t} \Delta_i^t H \cdot S_i \right. \\ & \left. + \sum_i C_{p_i}^L \cdot MW_i \cdot x_i^L \cdot (1 - S) \cdot \Delta T + \sum_i C_{p_i}^S \cdot MW_i \cdot x_i^S \cdot S \cdot \Delta T \right) \cdot \frac{1}{1S} \end{aligned} \quad (5)$$

$$\begin{aligned} DSC_{\text{theoretical}} = & \left(- \sum_i \Delta_i^p H \cdot S_i - \sum_i \Delta_i^t H \cdot S_i + \sum_i C_{p_i}^L \cdot MW_i \cdot x_i^L \cdot (1 - S) \cdot \Delta T \right. \\ & \left. + \sum_i C_{p_i}^S \cdot MW_i \cdot x_i^S \cdot S \cdot \Delta T \right) \cdot \frac{1}{1S} \end{aligned} \quad (6)$$

where $DSC_{\text{theoretical}}$ is the value of the calculated calorimetric curve; $\Delta_i^p H$ is the enthalpy of the solid-liquid transition of component i ; $\Delta_i^t H$ is the enthalpy of the solid-solid transition; $C_{p_i}^L$ and $C_{p_i}^S$ are the specific heat capacities of component i in the liquid and solid phases; MW_i is the molecular weight of component i ; and ΔT is the

temperature variation, considering a reference temperature; (1/1s) refers to a heating or cooling rate of ΔT per second, correspondent to 1K/s in this paper.

Since all the solid phases are pure in the MS approach, the term $x_i^S S$ is analogous to S_i in multisolid phase model, which means the amount of solid i . The solid-solid transition enthalpy in the MS model is taken into account only when the system is at a temperature below the solid-solid transition temperature of a given substance.

The solid-solid transition will not be accounted for when using the SS approach. Hence, in this approach the transition enthalpy is considered as the sum of fusion and solid-solid transition enthalpies for any precipitation.

The term $\Delta_i^p H$ in Equations (5) and (6) is related to the solid-liquid transition enthalpy that does not occur necessarily at the fusion temperature of pure component. Therefore, the fusion enthalpy has to be corrected as shown in Equation (7).

$$\Delta_i^p H = \Delta_i^f H + \int_{T_i^f}^{T_i^p} \Delta C p_i dT \quad (7)$$

In this work, the liquid phase will be represented by Flory Free Volume combined with UNIFAC residual term as suggested by Coutinho and Stenby (1996) [4]. In this model, the free-volume term was calculated as a function of the van der Waals volume and molar volume of each component. The van der Waals volume was calculated from the correlation proposed by Motoc and Marshall (1985) [27], and the molar volume was obtained from the correlations proposed by Won (1986) [1] or Marano and Holder (1997) [28], depending on the selected correlation ensemble.

Wilson activity coefficient model will be used for the solid phase in the SS approach, as introduced by the same authors [4]. The interaction parameters (λ_{ji}) of Wilson model were calculated as a function of the sublimation heat of the component with smaller carbon chain, as proposed by Coutinho and Stenby (1996) [4].

The comparison between properties predicted by correlations and the experimental values were quantified by the mean absolute error (MAE), as shown in Equation (8). This same Equation was used for WDT, WPC and solid compositions comparison.

$$MAE = \frac{\sum_{i=1}^{npt} |X_i^{exp} - X_i^{mod}|}{npt} \quad (8)$$

where X is the property of interest, npt is the number of data points and the superscripts *exp* and *mod* stand respectively for experimental and modeled.

The evaluation criterion to choose the best correlation set for replication of calorimetric curves is different from the above. Since the experimental calorimetric curve is usually not reported along with the mass of the sample, the direct comparison of curve points is

not possible. An objective function was developed in our previous work [26] for this comparison and is shown in Equation (9).

$$f_{obj} = 0.95 \frac{\|T_{peak}^{exp} - T_{peak}^{mod}\|}{\text{number of peaks}} + 0.03 \frac{\|T_{valley}^{exp} - T_{valley}^{mod}\|}{\text{number of valleys}} + 0.02 \frac{\|T_{intermediate}^{exp} - T_{intermediate}^{mod}\|}{\text{number of intermediate points}} + p \quad (9)$$

where f_{obj} is the objective function, T_{peak}^{exp} , T_{valley}^{exp} , and $T_{intermediate}^{exp}$ are respectively the peaks, valleys and intermediate points (temperature values) of an experimental calorimetric curve. T_{peak}^{mod} , T_{valley}^{mod} , and $T_{intermediate}^{mod}$ are respectively the peaks, valleys, and intermediate points of the modeled calorimetric curve. Finally, the parameter p refers to the penalty applied to the objective function when the number of peaks predicted is different from the number reported by experiments; p is equal to 1.5 times the difference between these numbers.

Thermophysical properties correlations evaluated

Several correlations can be found in literature for temperatures and enthalpies of fusion and solid-solid transition. Those evaluated in this work are reported in Table 1.

Table 1 – Correlations evaluated and their source.

Properties	Origin of Correlations Considered
Fusion Temperature	[1, 5, 7, 8, 10, 11, 13, 29, 30]
Solid-Solid Transition Temperature	[4, 5, 8, 9, 10, 11, 30]
Fusion Enthalpy	[1-3, 5, 7-11, 13, 29, 30]
Solid-Solid Transition Enthalpy	[4, 5, 8, 9, 11, 30, 31]

The choice of correlations for calculating the heat capacity difference between the solid and liquid phases of pure components ($\Delta^f C p_i$) has small effect on the ratio between solid and liquid fugacities, as pointed out by Ghanaei et al. (2012) [31]. For this reason we have not included $\Delta^f C p_i$ as a property to be evaluated in the present work.

Correlations comparison through pure components properties

The correlations for the temperatures and enthalpies of fusion and solid-solid transition presented in this article were compared to experimental values. Table 2 presents calculated values for fusion temperature, and also, the comparison with experimental data found in the literature. This comparison was done by mean absolute error (Equation (8)).

Table 2 – Deviations from experimental data from the literature and MAE of correlations used for fusion temperature prediction, in K.

	Exp. Values	[1]	[7]	[5]	[8]	[30]	[10]	[29]	[11]	[13]
C₁₀H₂₂	243.51 ^a	7.06	31.26	6.05	44.65	8.62	115.03	25.22	7.06	2.6
C₁₅H₃₂	283.07 ^a	-2.02	14.82	0.57	120.38	-0.03	0.02	9.37	-2.02	0.04
C₂₀H₄₂	309.58 ^a	-0.92	10.58	-0.25	0.25	0.02	-0.17	7.05	-0.92	5.37
C₂₅H₅₂	326.65 ^a	0.12	10.76	0.37	-0.16	0.01	-0.04	7.23	0.12	-0.03
C₃₀H₆₂	338.65 ^a	0.79	13.49	-0.03	-0.22	-0.07	0.13	8.55	0.79	17.28
C₃₂H₆₆	342.35 ^a	0.79	14.78	-1.68	-0.29	-0.29	0.27	9.07	2.65	19.12
C₃₅H₇₂	347.20 ^b	0.72	16.94	-6.65	-0.4	-0.59	-0.46	9.94	1.38	-0.47
C₃₆H₇₄	349.05 ^a	1.07	18.09	-8.76	-0.08	-0.29	0.87	10.63	1.41	22.33
C₄₀H₈₂	354.10 ^c	0.69	21.05	-24.51	-1.01	-0.77	0.17	11.75	0.11	23.51
C₅₀H₁₀₂	365.30 ^d	1.07	29.87	-118.92	-9.55	-0.02	-0.04	16.24	-0.14	19.49
C₆₀H₁₂₂	375.00 ^c	2.33	38.85	-335.11	-39.89	2.3	2.13	21.64	1.92	1.39
MAE		1.60	20.04	45.72	19.72	1.18	10.85	12.43	1.68	10.15

^a DIPPR [32]; ^b Garner *et al.* (1931) [33]; ^c NIST [34]; ^d Seyer *et al.* (1944) [35].

The same procedure was carried out for solid-solid transition temperature, fusion enthalpy, and solid-solid transition enthalpy, presented in Table 3 to 5.

Table 3 Deviations from experimental data from the literature and MAE of correlations used for the prediction of solid-solid transition temperature, in K.

	Exp. values	[4]	[5]	[8]	[30]	[10]	[9]	[11]
C₁₅H₃₂	270.93 ^a	1.23	0.53	2.77	0.67	0.33	4.87	1.03
C₂₀H₄₂	309.4 ^b	10.0	9.1	6.3	9.5	93.5	6.7	93.5
C₂₅H₅₂	320.0 ^c	0.5	0.1	3.1	0.4	2.6	0.1	0.5
C₃₀H₆₂	332.2 ^d	0.6	0.6	4.6	2.0	4.0	0.1	2.4
C₃₅H₇₂	344.7 ^d	2.6	3.1	2.2	0.7	4.7	2.9	0.0
MAE	-	3.0	2.7	3.8	2.7	21.0	2.9	19.5

^a Finke *et al.*, (1954) [36]; ^b Schaerer *et al.* (1955) [37]; ^c Barbillon *et al.* (1991) [38]; ^d Garner *et al.* (1931) [33]

Table 4 Deviations from experimental data from the literature and MAE for the prediction of fusion enthalpy, in kJ/mol.

	C ₁₀ H ₂₂	C ₁₅ H ₃₂	C ₂₀ H ₄₂	C ₂₅ H ₅₂	C ₃₀ H ₆₂	C ₃₂ H ₆₆	C ₃₆ H ₇₄	C ₄₀ H ₈₂	C ₅₀ H ₁₀₂	C ₆₀ H ₁₂₂	MAE
Exp. values	28.7 ^a	34.6 ^a	69.9 ^a	57.7 ^a	68.8 ^a	76.6 ^a	88.8 ^a	133 ^a	185 ^c	187 ^b	-
[1]	-8.7	1.3	-17.7	11.1	16.7	15.6	17.2	-14.0	-32.0	-8.7	13.5
[2]	-5.3	0.3	-23.6	0.1	0.4	-2.8	-5.8	-40.8	-70.0	-5.3	19.8
[3]	-18.4	-16.1	-43.0	-22.3	-24.8	-29.1	-34.4	-71.6	-106.0	-18.4	45.6
[7]	-21.3	-21.3	-50.6	-32.3	-37.2	-42.5	-49.7	-88.9	-128.2	-21.3	59.0
[5]	-9.8	0.1	-23.4	-0.8	-0.4	-2.6	-1.4	-28.0	-8.0	-9.8	19.3
[8]	-9.9	0.0	-23.4	-0.8	-0.4	-2.6	-1.4	-28.0	-8.0	-9.9	19.3

[30]	-9.7	0.1	-23.4	-0.5	0.4	-1.6	0.5	-25.0	0.0	-9.7	19.5
[9]	-3.8	10.1	-50.6	-32.3	-37.3	-42.6	-49.8	-89.0	-128.4	-3.8	56.2
[10]	-11.2	-2.1	-23.4	-0.8	-0.4	-2.6	-1.4	-28.0	-8.0	-11.2	19.6
[29]	-13.6	-7.5	-30.4	-5.7	-4.1	-6.9	-8.8	-42.8	-69.0	-13.6	23.4
[11]	-1.7	0.0	-30.4	-5.7	-4.1	-6.9	-8.8	-42.8	-69.0	-1.7	21.4
[13]	-21.3	-21.4	-50.6	-32.3	-37.3	-42.6	-49.8	-89.0	-128.4	-21.3	59.1

^a DIPPR [32]; ^b Lourdin *et al.* (1992) [39]; ^c Hammami and Mehrotra (1995) [40].

Table 5 – Deviations from experimental data from the literature and MAE for the prediction of solid-solid transition enthalpy, in kJ/mol.

	$C_{25}H_{52}$	$C_{30}H_{62}$	$C_{35}H_{72}$	MAE
Experimental values	26.5 ^a	36.5 ^b	41.1 ^b	-
[31]	-13.4	-21.1	-23.5	19.3
[9]	1.3	-2.0	0.2	1.2
[4]	-25.1	-34.6	-39.0	32.9
[5]	-2.1	-4.3	-6.2	4.2
[8]	-2.0	-3.2	-1.7	2.3
[30]	-1.8	-5.0	-6.8	4.5
[10]	-17.6	-16.2	-21.9	18.6
[11]	-1.3	1.9	-4.1	2.4

^a Barbillon *et al.* (1991) [38]; ^b Garner *et al.* (1931) [33].

The lowest MAE obtained for each property are shown in Table 6. Despite of the fact that n-paraffins have been a subject of study for many years, there is still a lack of experimental data for heavier n-alkanes, what may cause the selection of correlations that does not represent these components very well.

Table 6 – Correlations with the lowest mean average deviation (*MAE*) in comparison with experimental data found in the literature.

Property	Origin of Equation with lowest <i>MAE</i>
Fusion temperature	[30]
Solid-solid transition temperature	[30]
Fusion enthalpy	[1]
Solid-solid transition enthalpy	[9]

Correlations evaluation through Wax Dissolution Temperature

The individual analysis of a correlation is only possible by the comparison between calculated and experimental data of pure components. To evaluate their adequacy for the prediction of wax disappearance temperature and the amount of wax precipitated at each temperature, it is necessary to collect them, and in the present work this is done by

evaluating ensembles of correlations proposed by different authors, including the properties listed in Table 1 and $\Delta^f C p_i$, as presented in Table 7. For ensemble A, the correlation for $\Delta^f C p_i$ was of Pedersen and Skovborg (1991) [3].

Table 7 – Evaluated correlations ensembles.

Correlation ensembles	Origin
A	Equations with lower deviations from experimental pure component data (Table 6)
B	[13]
C	[11]
D	[31]
E	[41]
F	[29]
G	[42]
H	[10]
I	[43]
J	[9]
K	[30]
L	[8]
M	[44]
N	[5]
O	[7]
P	[3]
Q	[1]

Not all works explicit the correlations used for all the properties. In such cases, whenever required, a correlation from ensemble A – that contains equations with lowest mean average deviation in comparison with experimental data for pure compounds – will be used.

The mixtures selected for WDT comparison, their compositions and experimental wax dissolution temperatures are presented in Table 8 for SS model and Table 9 for MS.

Table 8 – Mixtures selected for WDT comparison by SS model.

% molar	Mixture 1	Mixture 2	Mixture 3
C ₆ H ₁₄	-	-	-
C ₁₆ H ₃₄	73.00	-	-
C ₁₇ H ₃₆	-	25.00	-
C ₁₈ H ₃₈	27.00	-	48.00
C ₁₉ H ₄₀	-	75.00	15.00
C ₂₀ H ₄₂	-	-	37.00
C ₂₈ H ₅₈	-	-	-

$C_{41}H_{84}$	-	-	-
WDT (K) ^a	292.00	302.00	304.00

^a Ji *et al.* (2004) [10]

Table 9 – Mixtures selected for WDT comparison by MS model.

% molar	Mixture 4	Mixture 5	Mixture 6
C_6H_{14}	75.40	79.30	-
$C_{16}H_{34}$	24.60	-	34.00
$C_{17}H_{36}$	-	20.70	-
$C_{18}H_{38}$	-	-	-
$C_{19}H_{40}$	-	-	-
$C_{20}H_{42}$	-	-	-
$C_{28}H_{58}$	-	-	32.00
$C_{41}H_{84}$	-	-	34.00
WDT (K)	275.00 ^a	274.00 ^a	348.95 ^b

^a Ji *et al.* (2004) [10]; ^b Paunovic and Mehrotra (2000) [45]

A comparison between experimental WDT data and values estimated by the MS and SS models using the various correlations ensembles was carried using Equation (8) to estimate the deviations. Three mixtures with components of similar size (Table 8) were chosen to evaluate the SS model, while for the MS model another three mixtures with larger size differences among their components (Table 9) were selected.

Table 10 and 11 shows WDT calculated with correlations ensembles A to Q for Mixtures 1 to 3 and and for Mixtures 4 to 6, respectively. Values outlined in these tables are within the reproducibility value (3.5 K) for liquid-solid transition established by ASTM D4419-90 (2015) [46].

Table 10 – Calculated WDT for Mixtures 1, 2 and 3 by SS model.

Correlations Ensemble	Mixture 1		Mixture 2		Mixture 3		Mixture 1, 2 and 3
	WDT	MAE	WDT	MAE	WDT	MAE	MAE
A	289.53	2.47	302.12	0.12	300.13	3.87	2.15
B	284.68	7.32	299.56	2.44	291.12	12.88	7.55
C	292.15	0.15	303.10	1.10	303.76	0.24	0.50
D	290.87	1.13	303.26	1.26	302.83	1.17	1.19
E	289.35	2.65	301.92	0.08	301.72	2.28	1.67
F	280.51	11.49	294.26	7.74	293.35	10.65	9.96
G	291.30	0.70	303.34	1.34	301.16	2.84	1.63
H	289.83	2.17	301.84	0.16	301.92	2.08	1.47
I	289.19	2.81	301.80	0.20	296.64	7.36	3.46
J	291.86	0.14	303.73	1.73	302.27	1.73	1.20
K	289.09	2.91	301.83	0.17	301.26	2.74	1.94
L	289.70	2.30	301.67	0.33	301.49	2.51	1.71
M	291.14	0.86	303.32	1.32	301.15	2.85	1.68

N	288.94	3.06	302.01	0.01	301.42	2.58	1.88
O	273.14	18.86	288.39	13.61	287.43	16.57	16.35
P	289.19	2.81	301.80	0.20	296.64	7.36	3.46
Q	291.17	0.83	303.32	1.32	301.17	2.83	1.66

Table 11 – Calculated WDT for Mixture 4, 5 and 6 by MS model.

	Mixture 4		Mixture 5		Mixture 6		Mixtures 4, 5 and 6
Correlations Ensemble	WDT	MAE	WDT	MAE	WDT	MAE	MAE
A	265.63	9.37	269.57	4.43	349.29	0.34	4.71
B	239.71	35.29	241.09	32.91	343.68	5.27	24.49
C	273.31	1.69	272.62	1.38	348.61	0.34	1.14
D	269.07	5.93	273.17	0.83	346.71	2.24	3.00
E	267.16	7.84	271.10	2.90	347.85	1.1	3.95
F	250.12	24.88	254.07	19.93	339.49	9.46	18.09
G	266.89	8.11	270.57	3.43	348.31	0.64	4.06
H	264.32	10.68	272.37	1.63	349.28	0.33	4.21
I	239.71	35.29	241.09	32.91	344.98	3.97	24.06
J	271.84	3.16	275.91	1.91	345.86	3.09	2.72
K	267.54	7.46	271.71	2.29	347.91	1.04	3.60
L	268.42	6.58	272.42	1.58	349.66	0.71	2.96
M	267.00	8.00	270.71	3.29	348.26	0.69	3.99
N	266.87	8.13	271.22	2.78	348.61	0.34	3.75
O	264.32	10.68	272.37	1.63	332.79	16.16	9.49
P	239.89	35.11	241.34	32.66	344.89	4.06	23.94
Q	267.20	7.80	270.91	3.09	348.32	0.63	3.84

As shown in Table 10, only ensembles B, F, and O for Mixture 1 and again F and O for Mixture 2 predicted a WDT outside the reproducibility criteria [46]. A larger number of ensembles predict a WDT outside ASTM reproducibility interval for Mixture 3: A, B, F, I, O, and P.

Ensembles B, F, I, O, and P have in common fusion enthalpies correlations that generate estimates that are lower than experimental data (see Table 4 together with Table 7). Fusion enthalpy correlation from ensemble O, was proposed by Lira-Galeana *et al.* (1996) [7] for petroleum cuts, being mentioned by the authors that components of same molar mass might present a variety of fusion enthalpies, and this is the reason why fusion enthalpy correlation suggested by Won (1986) [1] is not appropriate, since it overestimates the amount of precipitated wax bellow the cloud point temperature for petroleum mixtures. Thus, fusion enthalpy correlation from ensemble O was not able to produce good estimates when it was applied to n-paraffin mixtures. Fusion enthalpy correlation from ensemble F was developed by Escobar-Remolina (2006) [29] with the intention of being “multi-conceptual”, being settled as the average of previous correlations found in literature. From results reported in Table 10, it is possible to state that this correlation is not suitable for n-paraffin mixtures.

Furthermore, fusion temperatures equations from ensembles B, F, and O generate values well below the experimental ones (see Table 2 together with Table 7). Ensembles F and O are those that generated results with the largest errors for Mixtures 1, 2, and 3. Tabatabaei-Nejad and Khodapanah (2009) [13] noted that the most sensible input data

for WDT evaluation is fusion temperature, what may justify the great difference between WDT predicted by ensembles F and O from experimental values.

From Table 10, that presents MAE for WDT results corresponding to Mixtures 1, 2 and 3 and considering SS approach, it is possible to conclude that ensembles A, C, D, E, G, H, J, K, L, M, N, P, and Q were inside the reproducibility interval for liquid-solid transition [46]. However, only Ensembles C, D, J, and L were able to predict WDT values inside the reproducibility interval for Mixtures 4, 5 and 6, considering the MS approach, as presented in Table 11. Thus, these ensembles will be selected for further analysis. Ensemble A was also kept, because it presents correlations that predict pure n-alkane properties closest to experimental values.

As presented in Table 11, MAE for MS model predictions of WDT calculated for Mixtures 4 and 5 were significantly higher than the ones computed for Mixtures 1, 2, and 3 by SS model, and Mixture 6 by MS model. There are not many data available in the literature concerning experimental WDT values for n-paraffin mixtures with great size differences among their components, what reduced the evaluations options.

Additionally, ensembles with higher MAE (B, F, I, O, and P) for MS model are the same that generated the worst results for SS model. These ensembles, as stated before, possess correlations that predict low values for fusion enthalpies. Ensembles B, F, and O also underestimate significantly fusion temperature values.

The evaluation of the best correlation ensemble for SS model continues in the next section by comparing predicted WPC.

Evaluation of the correlations by the amount of wax precipitated at each temperature (WPC)

Table 12 presents the mixtures selected for WPC comparison. For all the mixtures studied decane acts as a solvent. Mixture 7 is composed further by 3 other n-paraffins with consecutive carbon atoms numbers from tetracosane to hexacosane while mixtures 8 to 10 contain a larger number of alkanes with consecutive carbon numbers. Mixtures 11 and 12 have bimodal distributions of n-alkanes with some difference in carbon chain size between the two groups.

Table 12 – Mixtures selected for WPC comparison by SS model.

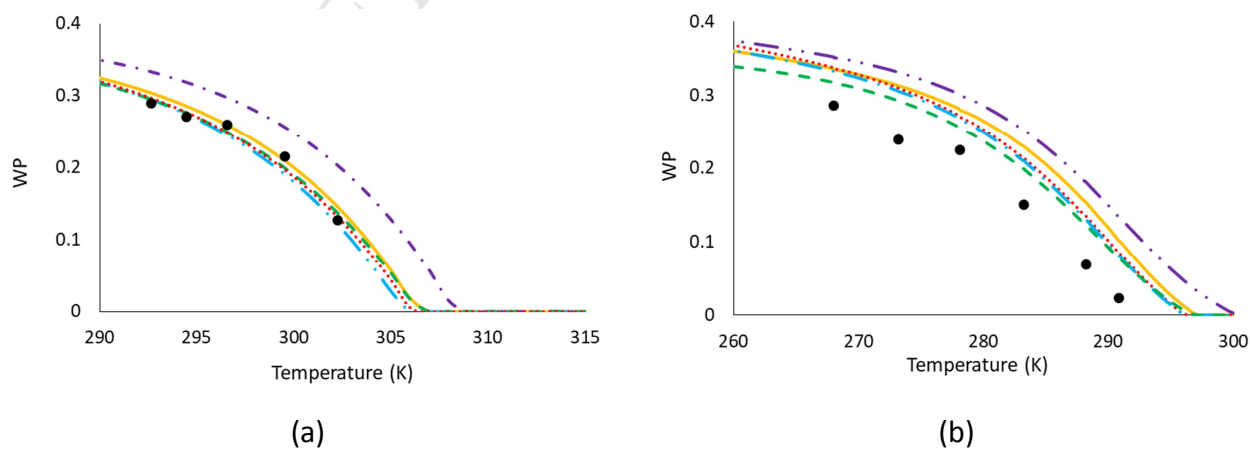
% molar	Mixture 7 ^a	Mixture 8 ^b	Mixture 9 ^b	Mixture 10 ^c	Mixture 11 ^c	Mixture 12 ^c
C ₁₀ H ₂₂	80.00	80.02	80.09	80.06	80.02	80.01
C ₁₈ H ₃₈	-	-	2.48	3.00	4.75	7.09
C ₁₉ H ₄₀	-	-	2.35	2.57	4.07	6.09
C ₂₀ H ₄₂	-	6.41	2.23	2.21	3.49	5.22
C ₂₁ H ₄₄	-	4.39	2.12	1.89	3.00	-
C ₂₂ H ₄₆	-	3.00	2.02	1.62	2.57	-

$C_{23}H_{48}$	-	2.05	1.92	1.39	-	-
$C_{24}H_{50}$	7.71	1.40	1.83	1.20	-	-
$C_{25}H_{52}$	6.62	0.96	1.74	1.03	-	-
$C_{26}H_{54}$	5.68	0.65	1.65	0.88	-	-
$C_{27}H_{56}$	-	0.45	1.58	0.76	-	-
$C_{28}H_{58}$	-	0.30	-	0.65	-	-
$C_{29}H_{60}$	-	0.21	-	0.56	-	-
$C_{30}H_{62}$	-	0.14	-	0.48	-	-
$C_{31}H_{64}$	-	-	-	0.41	-	-
$C_{32}H_{66}$	-	-	-	0.35	0.56	-
$C_{33}H_{68}$	-	-	-	0.30	0.48	-
$C_{34}H_{70}$	-	-	-	0.26	0.41	0.61
$C_{35}H_{72}$	-	-	-	0.19	0.35	0.53
$C_{36}H_{74}$	-	-	-	0.19	0.30	0.45

^a Pauly *et al.* (2004) [47]; ^b Pauly *et al.* (1998) [48]; ^c Dauphin *et al.* (1999) [49].

No WPC data for mixtures that would theoretically result in pure solid phases (with components of great size differences) were found in literature. For this reason, the best correlation ensemble used by MS model will not be analyzed in this section. It was observed that MS approach applied to Mixtures 7 to 12 underestimates WPC, what is consistent with findings reported by Esmaeilzadeh *et al.* (2006) [42]. These authors concluded that the SS approach better represents the systems that contain consecutive carbon atoms among their components, and that the MS model underestimates WPC.

Figure 1 presents the wax precipitation curves (WPC) generated by SS model for Mixtures 7 to 12 with correlations ensembles A, C, D, J, and L, where WP is the weight fraction of crystallized paraffins, i. e., the mass of solid divided by the total mass of the system.



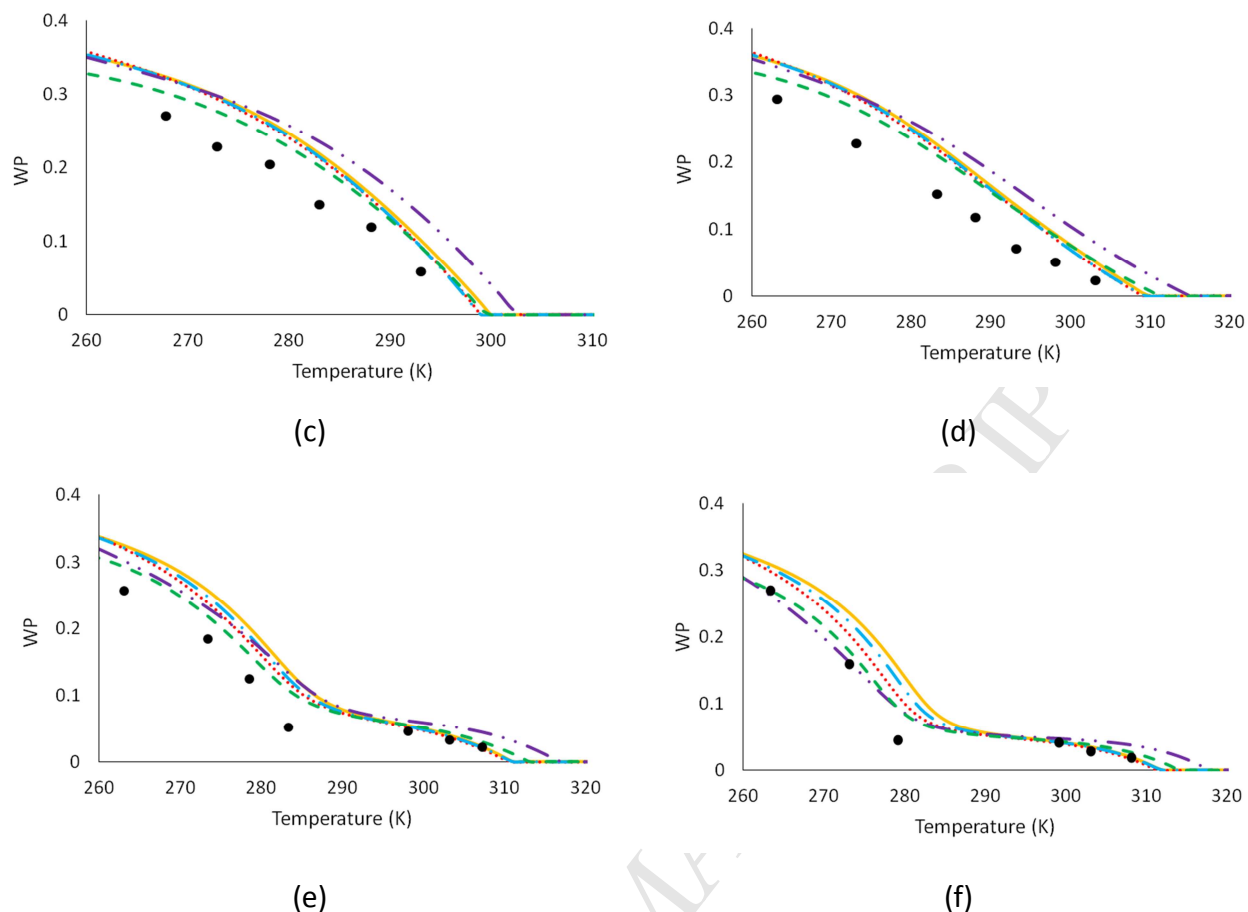


Figure 1 – WPC comparison between experimental values and values calculated using SS approach with Correlations Ensembles A, C, D, J, and L. (a) Mixture 7. (b) Mixture 8. (c) Mixture 9. (d) Mixture 10. (e) Mixture 11. (f) Mixture 12. (● : Experimental data ((a) [47]; (b) and (c) [48]; (d), (e) and (f) [49]); – · – · Ensemble A; — Ensemble C; ····· Ensemble D; — · — Ensemble J ; - - - Ensemble L).

For Mixtures 7 to 10, the correlation ensemble A produced poor agreement with experimental data, predicting a larger amount of precipitated solid than experimentally observed. Ensemble L leads to the lowest *MAE* for Mixtures 7 to 12, as it is shown in Table 13, which presents *MAE* calculated for Mixtures 7 to 12, comparing experimental and calculated data.

Table 13 – Comparison of WPC *MAE* (multiplied by 10^2) using the SS approach (Equation (8)) using Ensembles A, C, D, J, and L for Mixtures 7 to 12.

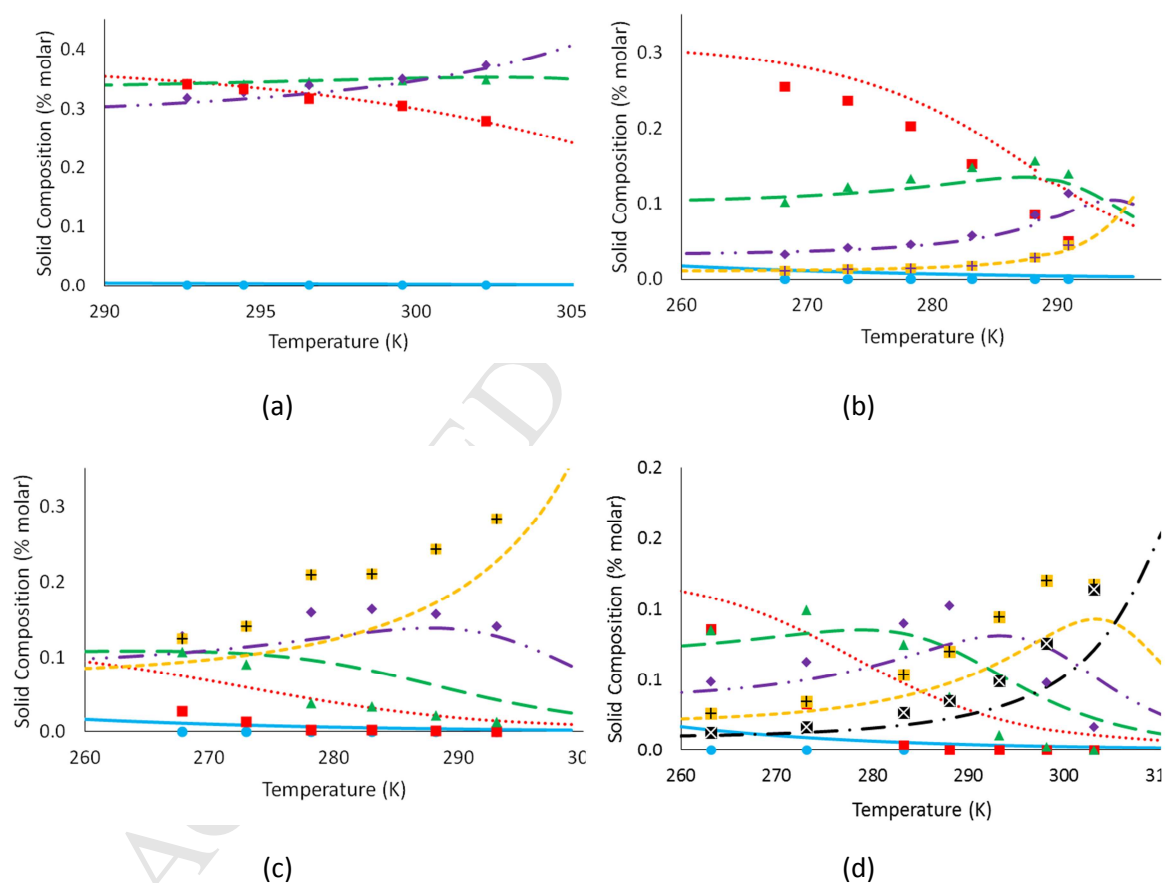
Ensemble	A	C	D	J	L
Mixture 7	2.29	0.58	0.49	0.60	0.46
Mixture 8	3.86	2.91	2.46	2.29	1.89
Mixture 9	2.86	2.29	2.08	2.14	1.62
Mixture 10	2.75	2.22	2.02	2.07	1.77
Mixture 11	1.74	2.16	1.71	1.90	1.20
Mixture 12	0.87	2.33	1.44	1.92	0.90
Mean	2.40	2.08	1.70	1.82	1.31

Regardless of the correlation ensemble used, SS approach using Wilson for the solid phase overestimated the amount of solid precipitated for Mixtures 8, 9 and 10, what is in agreement with the observations made by Coutinho *et al.* (2006) [50]. Wilson model was proposed for the solid n-paraffin phase by Coutinho *et al.* (1996) [51], with the

premise that the interaction energy between a long and a short molecule is the same as the interaction between two short molecules. Coutinho *et al.* (2006) [51] mentioned that this simplification was valid when the difference in size is not very significant, otherwise, the extremities of the long n-alkane will bend and further interactions between the molecules will arise. Thus, interactions between components of Mixtures 8 to 10 were probably neglected, resulting in higher amounts of solid precipitated.

Ensemble C was the one with poorest WPC predictions for Mixtures 11 and 12, and ensemble L the one with the best results for all tested mixtures.

A comparison of predicted solid compositions was also made. Figure 2 presents the comparison of solid compositions predicted by ensemble L that produced the best results for Mixtures 7 to 12. The comparison of predicted solid compositions for other ensembles is available at Supporting Information.



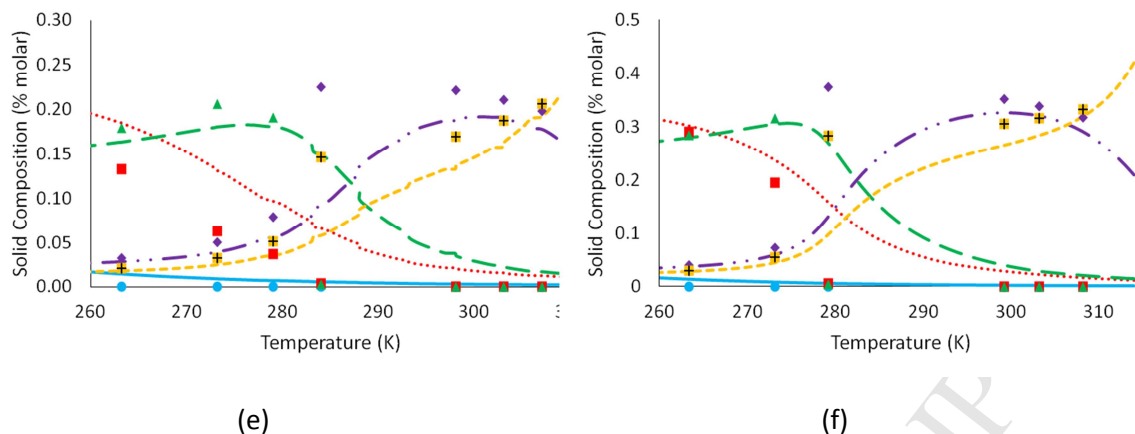


Figure 2 – Comparison of solid phase composition generated by SS model with experimental data for Mixture 7 to 12 with Correlations L. (a) Mixture 7 [47]. (b) Mixture 8 [48]. (c) Mixture 9 [48]. (d) Mixture 10 [49]. (e) Mixture 11 [49]. (f) Mixture 12 [49]. (a) Experimental: \bullet $C_{10}H_{22}$; \blacksquare $C_{24}H_{50}$; \blacktriangle $C_{25}H_{52}$; \blacklozenge $C_{26}H_{54}$. Modeled compositions: --- $C_{10}H_{22}$; --- $C_{24}H_{50}$; --- $C_{25}H_{52}$; --- $C_{26}H_{54}$. (b) Experimental: \bullet $C_{10}H_{22}$; \blacksquare $C_{20}H_{42}$; \blacktriangle $C_{23}H_{48}$; \blacklozenge $C_{26}H_{54}$; \boxplus $C_{29}H_{60}$. Modeled compositions: --- $C_{10}H_{22}$; --- $C_{20}H_{42}$; --- $C_{23}H_{48}$; --- $C_{26}H_{54}$; --- $C_{29}H_{60}$. (c) Experimental: \bullet $C_{10}H_{22}$; \blacksquare $C_{18}H_{38}$; \blacktriangle $C_{21}H_{44}$; \blacklozenge $C_{24}H_{50}$; \boxplus $C_{27}H_{56}$. Modeled compositions: --- $C_{10}H_{22}$; --- $C_{18}H_{38}$; --- $C_{21}H_{44}$; --- $C_{24}H_{50}$; --- $C_{27}H_{56}$. (d) Experimental: \bullet $C_{10}H_{22}$; \blacksquare $C_{19}H_{40}$; \blacktriangle $C_{23}H_{48}$; \blacklozenge $C_{27}H_{56}$; \boxplus $C_{31}H_{64}$; \boxtimes $C_{35}H_{72}$. Modeled compositions: --- $C_{10}H_{22}$; --- $C_{19}H_{40}$; --- $C_{23}H_{48}$; --- $C_{27}H_{56}$; --- $C_{31}H_{64}$; --- $C_{35}H_{72}$. (e) Experimental: \bullet $C_{10}H_{22}$; \blacksquare $C_{18}H_{38}$; \blacktriangle $C_{21}H_{44}$; \blacklozenge $C_{33}H_{68}$; \boxplus $C_{36}H_{74}$. Modeled compositions: --- $C_{10}H_{22}$; --- $C_{18}H_{38}$; --- $C_{21}H_{44}$; --- $C_{33}H_{68}$; --- $C_{36}H_{74}$. (f) Experimental: \bullet $C_{10}H_{22}$; \blacksquare $C_{18}H_{38}$; \blacktriangle $C_{20}H_{42}$; \blacklozenge $C_{34}H_{70}$; \boxplus $C_{36}H_{74}$. Modeled compositions: --- $C_{10}H_{22}$; --- $C_{18}H_{38}$; --- $C_{20}H_{42}$; --- $C_{34}H_{70}$; --- $C_{36}H_{74}$.

Ensemble A was the one with worst predictions of WPC for Mixture 7. They also lead to poor results for solid composition, as it can be seen in Figure 2 and Table 14, which shows the errors for the comparison between calculated and experimental solid compositions of Mixtures 7 to 12.

Table 14 – Comparison of solid composition generated by SS model with experimental data (Equation (8), with MAE multiplied by 10^2), in conjunction with Ensembles A, C, D, J, and L for Mixture 7 to 12.

Ensemble	A	C	D	J	L
Mixture 7	1.71	1.21	1.25	1.30	0.23
Mixture 8	0.87	7.20	0.43	0.44	0.60
Mixture 9	1.81	1.83	1.81	1.76	1.39
Mixture 10	1.27	1.15	1.12	1.08	0.95
Mixture 11	2.13	2.25	2.09	2.12	1.74
Mixture 12	3.60	4.20	3.85	4.02	3.20
Mean	1.90	2.97	1.76	1.79	1.35

According to Table 14, the best predictions for the composition of Mixture 7 were obtained by ensemble L, followed by ensembles C and D. Ensemble L was the one that predicted a decane composition closest to zero, consistent with experimental data of Mixture 7. Correlations used for fusion temperature estimation of this ensemble underestimate this property for decane, as can be observed in Table 2. This fact may have led to an error compensation between the SS approach employed and the values predicted by the correlations that are distant from experimental data of pure components.

Ensembles A and C were the ones with worse predictions of solid compositions for Mixtures 8 to 10. The best results were obtained by ensembles D (best prediction for Mixture 8), J, and L (best prediction for Mixtures 9 and 10).

Ensemble L had better predictions of WPC and solid compositions for Mixtures 11 and 12 (Table 13 and 14). Worse predictions were obtained by ensemble C, which only predicts the phenomena properly at higher temperatures. Ensemble A obtained good results of WPC for Mixtures 11 and 12, the opposite of what happened for the other mixtures. As it was previously exposed, Mixtures 11 and 12 present two groups of consecutive n-paraffins, with a significant size difference between the two groups.

From Tables 13 and 14 it is possible to state that the SS approach obtained better results with ensemble L, followed by ensembles D, and J, for WPC and solid compositions. Ensemble A had the worse results for Mixtures 7 to 10, and Ensemble C for Mixtures 11 and 12. The correlation ensembles analysis will continue through comparison of calorimetric curves with Ensembles D, J, and L, besides Ensemble A, that will be kept in the evaluation because it contains correlations that provide the best description of the experimental data of pure components.

Correlations evaluation by calorimetric curves

Six calorimetric curves were selected to evaluate the capability of the correlations ensembles together with SS and MS approaches to replicate them. The composition of the selected Mixtures is reported on Table 15.

Table 15 – Mixtures selected for calorimetric curves comparison by SS and MS approaches.

% molar	Mixture 13 ^a	Mixture 14 ^b	Mixture 15 ^c	Mixture 16 ^d	Mixture 17 ^d	Mixture 18 ^c
C ₁₆ H ₃₄	-	-	-	50.00	34.00	-
C ₁₈ H ₃₈	10.00	-	-	-	-	-
C ₂₀ H ₄₂	90.00	-	-	-	-	-
C ₂₂ H ₄₆	-	15.00	-	-	-	-
C ₂₃ H ₄₈	-	85.00	-	-	-	-
C ₂₄ H ₅₀	-	-	26.52	-	-	83.30
C ₂₆ H ₅₄	-	-	73.48	-	-	-
C ₂₈ H ₅₈	-	-	-	-	32.00	-
C ₄₀ H ₈₂	-	-	-	-	-	16.70
C ₄₁ H ₈₄	-	-	-	50.00	34.00	-

^a Fu *et al.* (2011) [52]; ^b Nouar *et al.* (1997) [53]; ^c Oliveira (1998) [54]; ^d Paunovic and Mehrotra (2000) (1999) [45].

Calorimetric curves for Mixtures 13, 14 and 15 were modeled by the SS approach since these mixtures present components with similar sizes. Figure 3 presents the comparison between experimental curves and the modeled ones using ensembles A, D, J, and L.

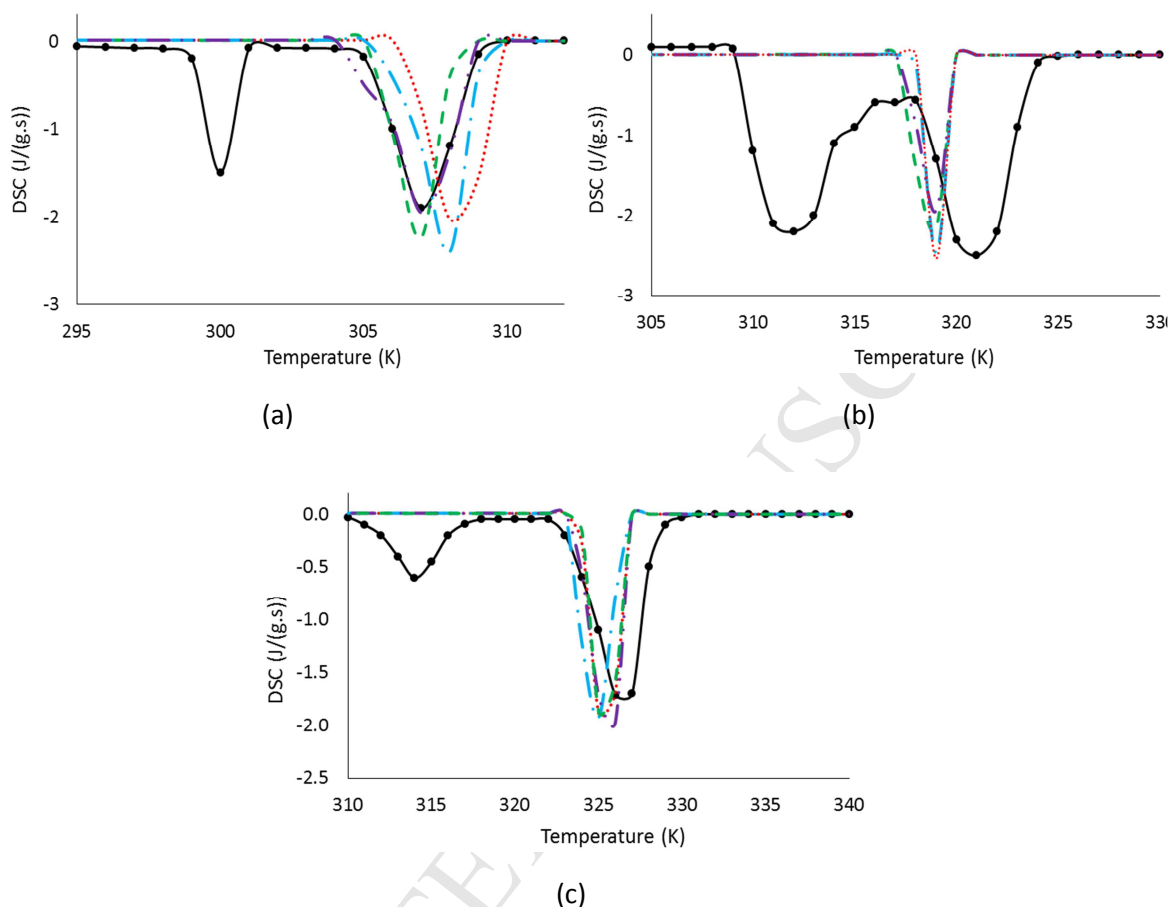


Figure 3 – Comparison of calorimetric curves generated by SS approach to experimental data. (a) Mixture 13. (b) Mixture 14. (c) Mixture 15. Experimental data by (a) Fu et al. (2011) [52], (b) Nouar et al. (1998) [53], and (c) Oliveira (1998) [54]. —●— Experimental curve; - - - Ensemble A; Ensemble D; - · - · Ensemble J; - - - Ensemble L.

It can be noticed that experimental curves on Figure 3 have two prominent peaks, related to liquid-solid and solid-solid transitions [52-54]. The calculated DSC curves have fewer peaks than the experimental ones. This was expected, since a premise for the SS approach adopted here is the direct transition from liquid phase to an ordered solid phase. The consideration of solid-solid transition on SS model and the possibility of formation of multiple solid solutions are being studied in order to consider these particularities in future works.

The peaks positions did not differ very much from one ensemble to another, having inclusive an overlap of ensembles D and J for Mixture 14 (Figure 3(b)). Another highlight is the position of the calculated curves in comparison with the experimental ones. The calculated peaks are at higher temperatures than the experimental for Mixture 13, whose DSC essay was performed with a cooling rate, and the calculated curves for Mixtures 14 and 15 are at lower temperatures than the experimental ones, whose experimental curves were measured on heating. This can be explained since in a DSC

measurement, the phase transition does not occur at real thermodynamic equilibrium, what may cause a delay in the position of thermic events when compared to the calculated, due to kinetic effects neglected in the model.

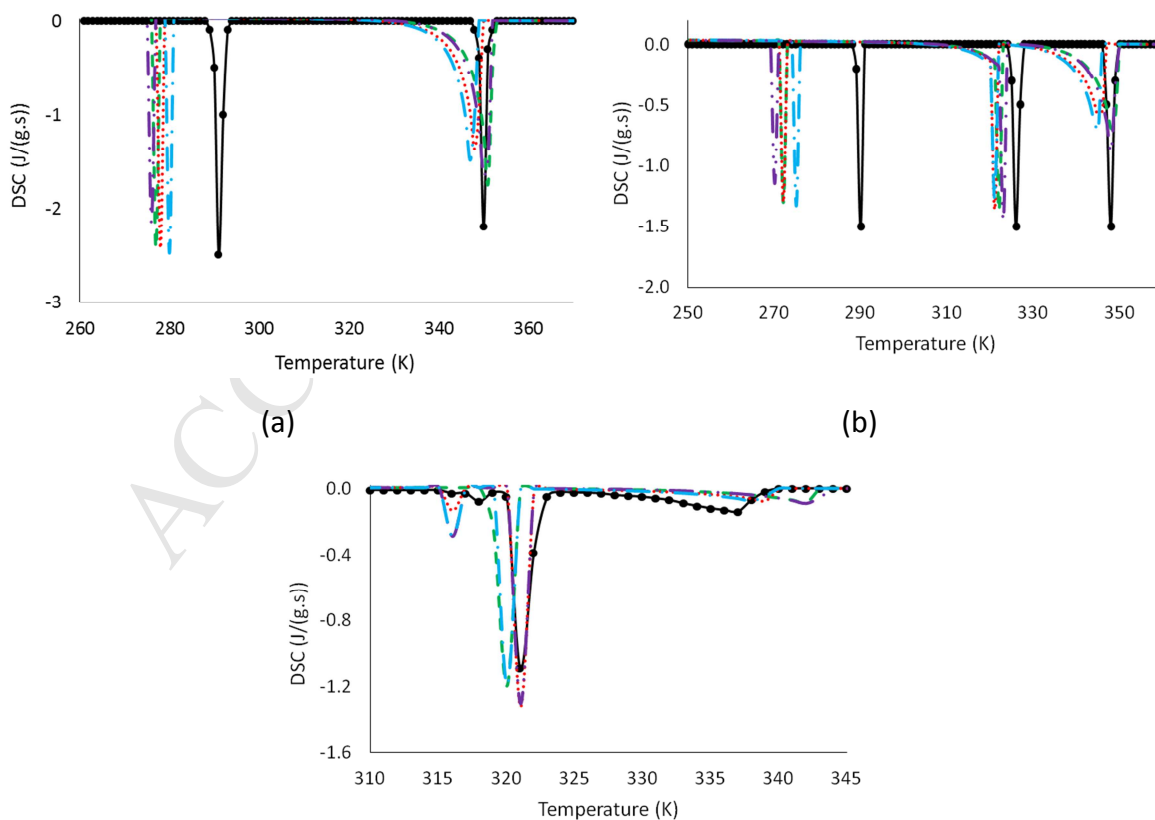
In order to compare the performance of ensembles A, D, J, and L, we used the objective function calculated by Equation (9). Results are presented in Table 16.

Table 16 – Objective functions calculated by Equation (9), comparing modeled calorimetric curves by SS approach with Ensembles A, D, J and L with experimental ones for Mixtures 13 [52], 14 [53] and 15 [54].

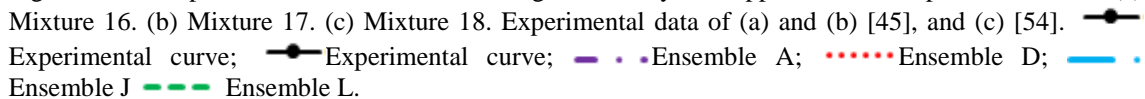




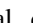
Ensemble	A	D	J	L
Mixture 13	1.6340	2.5697	2.5623	1.5063
Mixture 14	8.1964	8.1924	8.1927	8.2480
Mixture 15	1.6650	2.6148	2.6064	2.4630
Mean	3.8318	4.4590	4.4538	4.0724

The best description of the calorimetric curves was achieved with Ensembles A and L for the SS approach.

According to Petitjean et al. (2002) [22], only mixtures with great size differences among its components result in eutectic mixtures. For this reason, Mixtures 16 to 18 were selected for the next study, using MS model. Their calorimetric curves are presented in Figure 4.



(c)

Figure 4 – Comparison of calorimetric curves generated by MS approach with experimental data. (a) Mixture 16. (b) Mixture 17. (c) Mixture 18. Experimental data of (a) and (b) [45], and (c) [54].  Experimental curve;  Experimental curve;  Ensemble A;  Ensemble D;  Ensemble J  Ensemble L.

The experimental calorimetric curve of Mixture 16 presents two peaks, and the curve of Mixture 17 has three, all related to the solid-liquid transition of their components, as proposed by Paunovic and Mehrotra (2000) [45]. These authors observed that despite the size difference among components of Mixtures 16 and 17, the solid phases are not pure, what may explain the discrepancy in the position of the second peak of Mixture 16 (from higher to lower temperatures), and second and third peaks of Mixture 17.

Paunovic and Mehrotra (2000) [45] observed two peaks on the calorimetric curve of pure octacosane, related to solid-liquid and solid-solid transitions. However, the solid-solid transition of octacosane was not observed for Mixture 17, neither on the experimental nor on the calculated curve. There was no solid-solid transition prediction, since the correlations estimate these temperature transitions as varying from 328K (ensemble D) to 332K (ensemble L). These temperatures are above the solid-liquid transition for octacosane (second peaks of Figure 4 (b)). In other words, when octacosane precipitates, this component is already at a temperature below that of the solid-solid transition, crystallizing directly from the liquid to the orthorhombic phase.

The calorimetric curve of Mixture 18 presents 3 peaks, related, from right to left, to the solid-liquid transition of $C_{40}H_{82}$, the solid-liquid transition of $C_{24}H_{50}$, and solid-solid transition of tetracosane. Tetracontane may present itself in an orthorhombic or rotator form [17,18]. However, the transition temperatures calculated by the correlations vary from 350 K (ensemble J) to 356 K (ensemble L), values higher than the wax appearance temperature, occurring the direct transition from liquid to orthorhombic phase.

According to Mondieig *et al.* (2004) [21], tetracosane presents two rotator and one triclinic phases. However, the thermal effect from rotator-ordered phase transition is preponderant [14,19]. Therefore, only one solid-solid transition is observed in Figure 4 (c). The curves calculated with ensemble L predicted only the solid-liquid transition for tetracosane since the temperature of solid-solid transition estimated by the correlation is 320K for this ensemble, above the precipitation temperature. Other ensembles (A, D, and J) presented a third peak, because they estimate solid-solid transition at lower temperatures, between 316 and 317 K, which are below the precipitation of this component.

Although ensembles A, D, and J predicted the solid-solid transition for tetracosane, they were not able to predict its temperature properly. The difference observed might be related to the fact that the tetracosane solid phase is not pure, and as the DSC measurement was made in heating, this transition may occur at a temperature above the one that would be observed for a pure component.

Table 17 compares results obtained by Ensembles A, D, J, and L with MS approach, through Equation (9) for Mixtures 16 to 18.

Table 17 – Objective functions calculated by Equation (9), comparing modeled calorimetric curves by MS approach using ensembles A, D, J, and L with experimental ones for Mixtures 16 and 17 [45], and Mixture 18 [54].

Ensemble	A	D	J	L
Mixture 16	9.8927	8.9344	8.0273	9.4017
Mixture 17	7.7210	7.2780	6.3289	7.1274
Mixture 18	1.8910	1.0693	0.9591	4.1916
Mean	6.5016	5.7605	5.1051	6.9069

Ensembles D and J were those with minimum average value for objective function calculated by Equation (9), in comparison with experimental calorimetric curves for the MS approach. Ensembles D and J were those with worse results for the SS approach, considering the value of objective function in the comparison of the calorimetric curves. The results here reported show that the success of a correlation ensemble performance is highly dependent upon the thermodynamic approach used (MS or SS).

The performance of the correlations for pure components was the starting point of the procedure here proposed. In this first step the best correlations were collected in ensemble A. However, we have tested in the next step the performance of other correlations to predict properties that are important in the study of wax precipitation. In this case, as there are other effective parameters in the models used, we were testing if a compensation of errors could lead to the best results.

This way, the comparisons using the MS model were important to test the hypothesis of pure solids and also to check if the prediction of the activity coefficients of the liquid phase are good enough. As set A was not the best choice for MS this means that either the solids are not pure or the model used to calculate the activity coefficients of the liquid phase is not perfect. Further, by testing the SS model that eliminates the hypothesis of pure solid, we evaluated the prediction of activity coefficients of solid and liquid phases. As set A was not the best for all tests using SS as well, one may conclude that at least the model used for the liquid phase still does not perform perfectly, even if there are quite more studies for liquids than for solids in the literature.

Hence, the main message that we want to convey is that the problem is still open. This way, in this paper we show that the models need to be improved. Meanwhile we also showed the sets of correlation that give the best results in each case with the currently available tools.

Conclusions

Around 60 correlations for prediction of n-paraffin properties were evaluated, in order to select those that lead to better predictions of the wax precipitation using both the solid solution (SS) and multisolid (MS) approaches. After the comparison with thermophysical properties of pure components, the correlations were combined in 17 ensembles. The performance of these ensembles was evaluated comparing the

prediction of wax disappearance temperature (WDT), amount of wax precipitated (WPC), compositions of solid phase and calorimetric curves, with SS and MS approaches.

After WDT comparison, it was concluded that ensembles with correlations that generated lower values of temperature and enthalpy of fusion were those with worst predictions: B [13], F [29], and O [7].

For WPC curves by SS approach, the best ensemble was L [8], followed by ensembles D [55], and J [9]. For calorimetric curves using the SS approach, the best predictions were obtained by Ensembles A (equations with minor MAE in comparison with experimental data of pure components), and L. After the comparison of calorimetric curves by the MS approach, ensemble J produced the best results. Therefore, the successful performance of a correlation ensemble seems to depend upon the thermodynamic approach used (MS or SS) due to compensation of errors.

Although an extensive study of correlations was done, it is hard to determine which one is the best ensemble for all situations. Observing the ensembles quoted above, it can be noticed that ensembles A, D, J and L produced good results. Thus, their use is recommended in the prediction of the n-paraffin precipitation phenomena, by SS and MS approaches.

Acknowledgments

The authors thank Brazilian Agencies CNPq and FAPERJ for financial support.

List of Symbols

C_p – specific heat capacity

ΔH – enthalpy variation

\hat{f} – fugacity of component in solution

f – fugacity of pure component

f_{obj} – objective function

K – equilibrium constant

MW – molecular weight

n – number of carbon atoms

n_{pt} – number of points

P – pressure

R – gas universal constant

S – solid phase ratio

T – temperature

x – molar fraction

X – generic property

z – feed composition

Greek Letters

γ – activity coefficient

ϕ – fugacity coefficient of pure component

$\hat{\phi}$ – fugacity coefficient of component in solution

ψ – fugacity ratio between pure components in solid and liquid phases

Subscripts

i – component number

Superscripts

exp – experimental

f – fusion

L – liquid

mod – thermodynamic modeled

p – precipitation

S – solid

t – solid-solid transition

tot – total

References

- [1] K.W. Won, Thermodynamics for Solid Solution-Liquid-Vapor Equilibria: Wax Phase Formation from Heavy Hydrocarbon Mixtures, *Fluid Phase Equilib.* 30 (1986) 265-279.
- [2] K.W. Won, Thermodynamic Calculation of Cloud Point Temperatures and Wax Phase Compositions of Refined Hydrocarbon Mixtures, *Fluid Phase Equilib.* 53 (1989) 377-396.
- [3] K.S. Pedersen, P. Skovborg, Wax Precipitation from North Sea Crude Oils. 4. Thermodynamic Modeling, *Energy & Fuels* 5 (1991) 924-932.

- [4] J.A.P. Coutinho, E.H. Stenby, Predictive Local Composition Models for Solid/Liquid Equilibrium in n-Alkane Systems: Wilson Equation for Multicomponent Systems, *Ind. Eng. Chem. Res.* 35 (1996) 918-925.
- [5] J.A.P. Coutinho, Predictive UNIQUAC: A New Model for the Description of Multiphase Solid-Liquid Equilibria in Complex Hydrocarbon Mixtures, *Ind. Eng. Chem. Res.* 37 (1998) 4870-4875.
- [6] R.A. Heidemann, J. Madsen, E.H. Stenby, S.I. Andersen, Wax Precipitation Modeled with Many Mixed Solid Phases, *AIChE J.* 51 (2005) 298-308.
- [7] C. Lira-Galeana, A. Firoozabadi, J.M. Prausnitz, Thermodynamics of Wax Precipitation in Petroleum Mixtures, *AIChE J.* 42 (1996) 239-248.
- [8] J.A.P. Coutinho, A Thermodynamic Model for Predicting Wax Formation in Jet and Diesel Fuels, *Energy & Fuels* 14 (2000) 625-631.
- [9] D.V. Nichita, L. Goual, A. Firoozabadi, Wax Precipitation in Gas Condensate Mixtures, *SPE Prod. Facil.* 16 (2001) 250-259.
- [10] H.Y. Ji, B. Tohidi, A. Danesh, A.C. Todd, Wax phase equilibria: developing a thermodynamic model using a systematic approach, *Fluid Phase Equilib.* 216 (2004) 201-207.
- [11] W. Chen, Z. Zhao, X. Zhang, L. Wang Thermodynamic Phase Equilibria of Wax Precipitation in Crude Oils, *Fluid Phase Equilib.* 255 (2007) 31-36.
- [12] M.R. Rahimpour, M. Davoudi, S.M. Jokar, I. Khoramdel, A. Shariati, M.R. Dehnavi, Wax formation assessment of condensate in South Pars gas processing plant sea pipeline (a case study), *J. Nat. Gas Sci. Eng.* 10 (2013) 25-40.
- [13] S.A. Tabatabaei-Nejad, E. Khodapanah, An Investigation on the Sensitivity Analysis of the Parameters of Proposed Wax Precipitation Model, *Petrol. Sci. Technol.* 68 (2009) 89-98.
- [14] M. Dirand, M. Bouroukba, A.J. Briard, V. Chevallier, D. Petitjean, J.P. Corriou, Temperatures and enthalpies of (solid + solid) and (solid +liquid) transitions of n-alkanes, *The J. Chem. Thermodyn.* 34 (2002) 1255- 277.
- [15] P.M. Ghogomu, M. Bouroukba, J. Dellacherie, D. Balesdent, M. Dirand, On the ideality of liquid mixtures of long-chain n-alkanes, *Thermochimica acta* 306 (1997) 68-71.
- [16] A.R. Gerson, K.J. Roberts, J.N. Sherwood, A.M. Taggart, The role of growth environment on the crystallization of normal alkanes in the homologous series from C₁₈H₃₈ to C₂₉H₆₀, *J. Cryst. Growth* 128 (1993) 1176-1181.
- [17] M.G. Broadhurst, An Analysis of the solid phase behavior of normal paraffins, *Journal of Research* 66A (1962) 241-249.
- [18] W.R. Turner, Normal Alkanes, *Ind. Eng. Chem. Prod. Res. Develop.* 10 (1971) 238-260.
- [19] V. Chevallier, M. Bouroukba, D. Petitjean, D. Barth, P. Dupuis, M. Dirand, Temperature and Enthalpies of Solid-Solid and Melting Transitions of the Odd-Numbered n-Alkanes C₂₁, C₂₃, C₂₅, C₂₇, and C₂₉, *J. Chem. Eng. Data* 46 (2001) 1114-1122.
- [20] R.R. Matheson, P. Smith, A simple thermodynamic analysis of solid-solution formation in binary systems of homologous extended-chain alkanes, *Polymers* 26 (1985) 288-292.

- [21] D. Mondieig, F. Rajabalee, V. Metivaud, N-alkane Binary Molecular Alloys, *Chem. Mater.* 16 (2004) 786-798.
- [22] D. Petitjean, M. Pierre, P. Goghomu, M. Bouroukba, M. Dirand, Structural behavior of molecular alloys: n-pentacontane (n-C₅₀H₁₀₂)-n-pentacosane (n-C₂₅H₅₂); n-pentacontane(n-C₅₀H₁₀₂)-n-tricosane (n-C₂₃H₄₈) at room temperature, *Polymer* 43 (2002) 345-349.
- [23] E.P. Gilbert, P.A. Reynolds, A.S. Brown, J.W. White, N-Paraffin Solid Solutions: Modification of Phase Separation with Carbon Number, *Chem. Phys. Lett.* 255 (1996) 373-377.
- [24] J.M. Prausnitz, R.N. Lichtentaler, E. Gomes De Azevedo, *Molecular Thermodynamics of Fluid Phase Equilib.*, third ed., Pentice-Hall, 1999.
- [25] M.L. Michelsen, The Isothermal Flash Problem. Part I. Stability, *Fluid Phase Equilib.* 9 (1982) 1-19.
- [26] P.R. Kazmierczak, M.L.L. Paredes, E.R.A. Lima, Enhancing the objective function used to predict the composition of n-paraffin mixtures from calorimetric curves, *Thermochimica acta* 650 (2017) 56-65.
- [27] I. Motoc, G.R. Marshall, van der Waals volume fragmental constants, *Chem. Phys. Lett.*, 116 (1985), 415 – 419.
- [28] J.J. Marano, G.D. Holder, General equation for correlating the thermophysical properties of n-paraffins, n-olefins, and other homologous series. 2. asymptotic behavior correlations for pvt properties, *Ind. Eng. Chem. Res.*, 36 (1997), 1895-1907.
- [29] J.C.M. Escobar-Remolina, Prediction of Characteristics of Wax Precipitation in Synthetic Mixtures and Fluids of Petroleum: A New Model, *Fluid Phase Equilib.* v. 240 (2006) 197-203.
- [30] J.A.P. Coutinho, J.L. Daridon, Low Pressure Modeling of Wax Formation in Crude Oils, *Energy & Fuels* 15 (2001) 1454-1460.
- [31] E. Ghanaei, F. Esmailzadeh, J. Fathikaljahi, A new predictive thermodynamic model in the wax formation phenomena at high pressure condition, *Fluid Phase Equilib.* 254 (2007) 126–137.
- [32] DIPPR, Project 801, evaluated process design data, public release documentation, in: Design Institute for Physical Properties (DIPPR), American Institute of Chemical Engineers (AIChE), New York, 2014.
- [33] W.E. Garner, K. van Bibber, A.M. King, The melting points and heats of crystallization of the normal long-chain hydrocarbons, *J. Am. Chem. Soc.* 0 (1931) 1533-1541.
- [34] National Institute of Standards and Technology, U.S. Department of commerce, NIST standard reference Database 69: NIST chemistry WebBook. <http://webbook.nist.gov/chemistry/>
- [35] W.F. Seyer, R.F. Patterson, J.L. Keays, The Density and Transition Points of the n-Paraffin Hydrocarbons, *J. Am. Chem. Soc.* 66 (1944) 179-82.
- [36] H.L. Finke, M.E. Gross, J.F. Messerly, G. Waddington, Benzothiophene: heat capacity. Heat of Transition. Heat of Fusion and Entropy. An Order-Disorder Transition, *J. Am. Chem. Soc.* 76 (1954) 854-857.
- [37] A.A. Schaerer, C.J. Busso, A.E. Smith, L.B. Skinner, Properties of pure normal alkanes in the C₁₇ to C₃₆ range, *J. Am. Chem. Soc.* 77 (1955) 2017-2019.

- [38] P. Barbillon, L. Schuffenecker, J. Dellacherie, D. Balesdent, M. Dirand, Variation d'enthalpie subie de 260 K a 340 K par les 11-paraffines. comprises entrel' octadecane et l'hexacosane, *J. chim. Phys. Phys.-Chim. Biol.* 88 (1991) 91-113.
- [39] D. Lourdin, A.H. Roux, J.-P.E. Grolier, J.-M. Buisine, Thermobarometric and differential scanning calorimetric study of the polymorphism of some even and odd paraffins (C26, C27, C40, C60), *Thermochimica acta* 204 (1992) 99-110.
- [40] A. Hammami, A.K. Mehrotra, Liquid-solid-solid thermal behavior of n-C44H90+n-C50H102 and n-C25H52+n-C28H58 paraffinic binary mixtures, *Fluid Phase Equilib.* 111 (1995) 253-272.
- [41] J.A.P. Coutinho, B. Edmonds, T. Moorwood, R. Szczepanski, X. Zhang, Reliable Wax Predictions for Flow Assurance, *Energy & Fuels* 20 (2006) 1081-1088.
- [42] F. Esmaeilzadeh, J.F. Kaljahi, E. Ghanaei, Investigation of Different Activity Coefficient Models in Thermodynamic Modeling of Wax Precipitation, *Fluid Phase Equilib.* 248 (2006) 7-18.
- [43] Y. Sofyan, A.J. Ghajar, K.A.M. Gasem, A Systematic Method to Predict Cloud Point Temperature and Solid Precipitation, *Petrol. Sci. Technol.* 21(2003) 409-424.
- [44] M. Vafaie-Sefti, S.A. Mousavi-Dehghani, M.M. Bahar, Modification of Multisolid Phase Model for Prediction of Wax Precipitation: A New and Effective Solution Method, *Fluid Phase Equilib.* 173 (2000) 65-80.
- [45] I. Paunovic, A.K. Mehrotra, Liquid-solid phase transformation of C16H34, C28H56 and C41H84 and their binary and ternary mixtures, *Thermochimica acta* 356 (2000) 27-38.
- [46] ASTM D4419-90, Standard Test Method for Penetration of Bituminous Materials. American Society for Testing and Materials, 2015.
- [47] J. Pauly, J.L. Daridon, J.A.P. Coutinho, Solid deposition as a function of temperature in the nC10+(nC24- nC25- nC26) system, *Fluid Phase Equilib.* 224 (2004) 237-244.
- [48] J. Pauly, C. Dauphin, J.L. Daridon, Liquid-solid equilibria in a decane+multi-paraffins system, *Fluid Phase Equilib.* 149 (1998) 191-207.
- [49] C. Dauphin, J.L. Dauridon, J.A.P. Coutinho, P. Baylèrec, M. Potin-Gautier, Wax content measurements in partially frozen paraffinic systems, *Fluid Phase Equilib.* 161 (1999) 135-151.
- [50] J.A.P. Coutinho, F. Mirante, J. Pauly, A New Predictive UNIQUAC for Modeling of Wax Formation in Hydrocarbon Fluids, *Fluid Phase Equilib.* 247 (2006) 8-17.
- [51] J.A.P. Coutinho, K. Knudsen, S.I. Andersen, E.H. Stenby, A Local Composition Model for Paraffinic Solid Solutions, *Chem. Eng. Sci.* 51 (1996) 3273-3282.
- [52] D. Fu, Y. Liu, Y. Su, G. Liu, D. Wang, Crystallization Behavior of Binary Even-Even n-Alkane Mixtures in Microcapsules: Effect of Composition and Confined Geometry on Solid-Solid Phase Separation, *J. Phys. Chem.* 115 (2011) 4632-4638.
- [53] H. Nouar, D. Petitjean, J.-B. Bourdet, M. Bouroukba, M. Dirand, Diagram of the n-tricosane-n-tetracosane mixtures: Corrections, *Thermochimica acta* 293 (1997) 87-92.
- [54] A.P. Oliveira, Estudo Experimental e Modelagem Termodinâmica da Precipitação de Parafinas em Sistemas Modelos, M.Sc. Dissertation, Universidade Estadual de Campinas, 1998.

- [55] E. Ghanaei, F. Esmailzadeh, J. Fathikaljahi, New Multi-Solid Thermodynamic Model for the Prediction of Wax Formation, *Int. J. Chem. Biol. Eng.* 1 (2008) 44-49.

ACCEPTED MANUSCRIPT